GA–A26737

3D-DIVIMP(HC) CODE MODELING OF DIII-D DiMES POROUS PLUG INJECTOR EXPERIMENTS

by

Y. MU, J.D. ELDER, P.C. STANGEBY, and A.G. McLEAN

JULY 2010

GENERAL ATOMICS

DISCLAIMER

GA–A26737

3D-DIVIMP(HC) CODE MODELING OF DIII-D DiMES POROUS PLUG INJECTOR EXPERIMENTS

by
Y. MU,* J.D. ELDER,† P.C. STANGEBY,† and A.G. McLEAN‡

This is a preprint of a paper to be presented at the Nineteenth International Conference on Plasma Surface Interactions, May 24-28, 2010, in San Diego, California, and to be published in the *Proceedings.*

*University of California-San Diego, La Jolla, California.
†University of Toronto Institute for Aerospace Studies, Toronto, Canada.
‡Oak Ridge National Laboratory, Oak Ridge, Tennessee.

Work supported by
the U.S. Department of Energy under
DE-FC02-04ER54698, DE-FG02-04ER54758,
DE-FG02-07ER54917, and DE-AC05-00OR22725

GENERAL ATOMICS PROJECT 30200
JULY 2010

GENERAL ATOMICS

ABSTRACT

A Porous Plug Injector (PPI) system for the Divertor Material Evaluation System (DiMES) on DIII-D has been employed for *in situ* study of chemical erosion in the tokamak divertor environment. The 3D-DIVIMP(HC) code has been applied to the interpretation of the CI, CII and other spectroscopic measurements made at the PPI location, for (a) the synthetic source due to injection of CH_4 through the PPI, and (b) the natural emission from the PPI head itself, which was inserted above surrounding graphite tiles by ~ 0.3 mm.

The code successfully replicated the MDS (spectrometer)-measured absolute emissions of CH, CI, CII 427 nm, 514 nm, and 658 nm and the DiMES TV-measured spatial shapes of the CH, CI, and CII 514 nm emission "clouds" to within the combined uncertainties. It is thus concluded that the most important physics and chemistry of chemical sputtering have most likely been included in the model.

I. INTRODUCTION

Carbon plasma-facing surfaces in tokamaks are subject to chemical erosion due to hydrocarbon formation. Understanding chemical erosion and molecular break up in current tokamaks is important for making projections of tritium inventory in reactors due to codeposition. This understanding can be developed by applying models of hydrocarbon breakup and transport to the interpretation of spectroscopic observations of emissions resulting from hydrocarbons entering the plasma. This task was made easier by the Porous Plug Injector (PPI) system developed by A.G. McLean and J.W. Davis [1] for use with DiMES [2] on DIII-D to admit methane (or other hydrocarbon gases) through a porous graphite surface, so that the molecular interaction with the plasma closely approximates a hydrocarbon molecule released from a carbon surface by chemical erosion. Injecting methane at a known rate provides direct calibration of spectroscopic signals from the Multichord Divertor Spectrometer (MDS) and the DiMES TV camera which view DiMES from above [3]. We report here on the simulation of the CI, CII and other spectroscopic measurements made at the PPI location, for (a) the synthetic source due to injection of CH_4 through the PPI, and (b) the natural emission from the leading edge of the unintentionally misaligned PPI head.

II. MODELING THE PPI PUFF

The 3D-DIVIMP(HC) [4] code was used to simulate the puffed CH, CI and CII emissions measured during the 2007 PPI experiment, performed in an attached L-mode plasma with $T_e \sim 25$ eV and $n_e \sim 1.5 \times 10^{19}$ m^{-3} varying radially at the PPI location. Data were taken from several repeat shots. A series of cases was run to model the DiMES TV-measured CH 427.0 – 431.5 nm, CI 908.9 nm, and CII 514.3 nm *toroidal profiles* and the MDS-measured CH 427.0 – 431.5 nm, CI 908.9 nm, CII 426.7 nm, CII 514.3 nm, and CII 658.0 nm *absolute emissivities*.

For the case represented here, 3D-DIVIMP(HC) launches CH_4 at a single, representative puff rate ($3.8 \times 10^{17} CH_4$ /s, deduced by the volume of the gas canister and the pressure change monitored during the shots, with an estimated error of 3% [3]) distributed uniformly across the holed PPI head surface (a circle of radius 0.015 m in the R-T plane, centered at z = 0.0 m). The initial velocity of the launched CH_4 was 650 m/s (0.0027 eV, corresponding to thermalization with a 300 K surface temperature) vertically in the +z direction [4]. The Janev-Reiter (JR) Database [5] [6] [7] is utilized to model the hydrocarbon evolution processes, until the CH_4 evolve into C^{2+}. All hydrocarbons striking the target are reflected back into the plasma assuming the Jacob hydrocarbon reflection coefficients (or alternative sticking coefficients) database [8]. For these shots B = 2.24 T and the pitch angle = 0.9 deg between B and the solid surface at the Outer Strike Point (OSP). Larmor rotation induced prompt redeposition and the effect of the MPS are included.

A. The spatial molecular/particle distribution for three spectroscopic bands/lines

The CD/CH distribution measured by DiMES TV in Shot 129689 is shown in Fig. 1. The edge of the PPI and the emission from the puffed CH_4 are clearly visible in the middle of the picture. Emission coming from the strike point region where the plasma surface interaction is the strongest and at tile edges is also clearly visible. There is an notable emission from the upstream (direction facing into the plasma flow) edge of DiMES due to a small unplanned misalignment of the sample holder. The 3D-DIVIMP(HC) simulation of the CH band emission is shown in Fig. 2. This result models only the puffed CH_4 and so does not reproduce the band of naturally occurring emission corresponding to the strike point position or tile edges. In order to make quantitative comparisons of the toroidal profile through the center of the emission cloud, a toroidal arc composed of 8 pixels in the radial direction in the DiMES TV picture (~ 6 mm wide) is extracted, averaged and plotted against the 3D-DIVIMP(HC) emission

for the same region (red profile in Fig. 3); the upstream spike aside, 3D-DIVIMP(HC) matches the experimental shape of the gas puff quite well. The minor peak showing up in the upstream side of the experimental measurement is due to the plasma interaction at the upstream edge of the slightly misaligned PPI porous cap (Fig. 4); a detailed simulation of this secondary peak caused by the PPI head misalignment is given in Sec. III. The red profile in Fig. 5 shows the normalized CI toroidal profiles from the DiMES TV measurement and 3D-DIVIMP(HC) simulation; the slightly unintentionally misaligned PPI head also causes a spike in upstream direction clearly visible at this wavelength. The CII 514 nm distribution was measured by DiMES TV in Shot 129691; in the downstream direction some of the CII emission from the puff is 'lost' due to the absence in natural CII emission at the trailing edge gap of DIMES; to compensate, an estimated increment has been added to the experimental profile. Toroidal profiles of normalized results are compared in Fig. 6 (red) and found to agree approximately in shape. There are several variables that affect the length of the downstream emission tail. These include the loss rate of carbon particles and the amount of time they have to couple to the background plasma flow. These dependencies are included in the model.

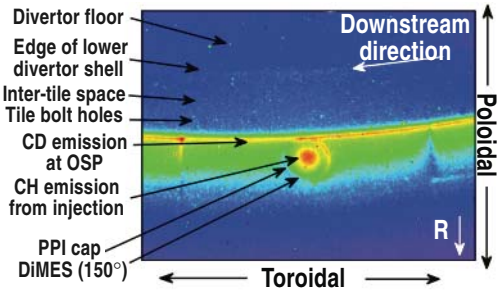

Fig. 1. DiMES TV view of the PPI in CH/CD light showing the light from the puff, at the center of DiMES. The bright arc at the upstream edge of the DiMES head is due to a slight vertical misalignment.

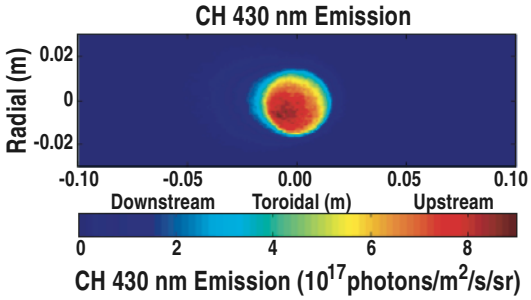

Fig. 2. CH 430.0 nm band emission 2D simulation from 3D-DIVIMP(HC).

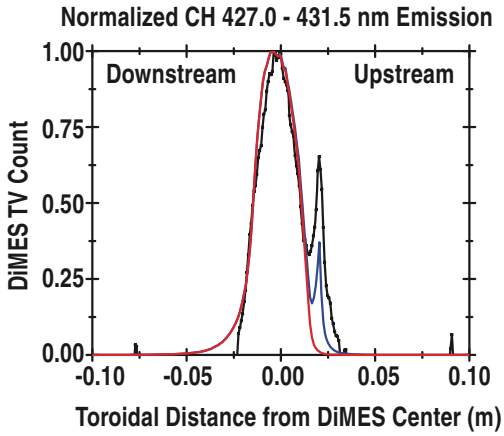

Fig. 3. CH 427.0 – 431.5 nm profile comparison. Experiment measurement: black. Code calculation: red (only the puff signal) and blue (both the puff and leading edge sputtering signals). Shot 129689. Code for 20 eV, 1.2 $\times 10^{19}$ m^{-3}.

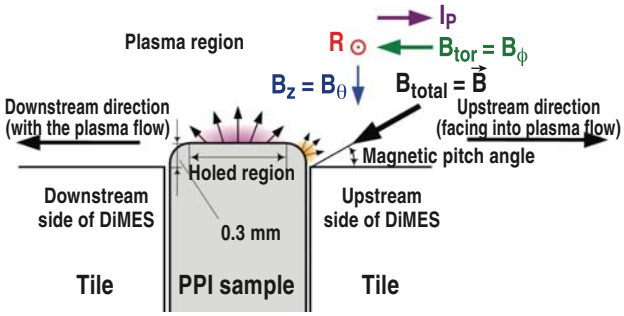

Fig. 4. Unintended misalignment of PPI head (~0.3 mm too high) caused an obvious, enhanced plasma interaction at the exposed edge. Fortunately this did not compromise the experiment. It also provided a convenient check of the background plasma flow direction.

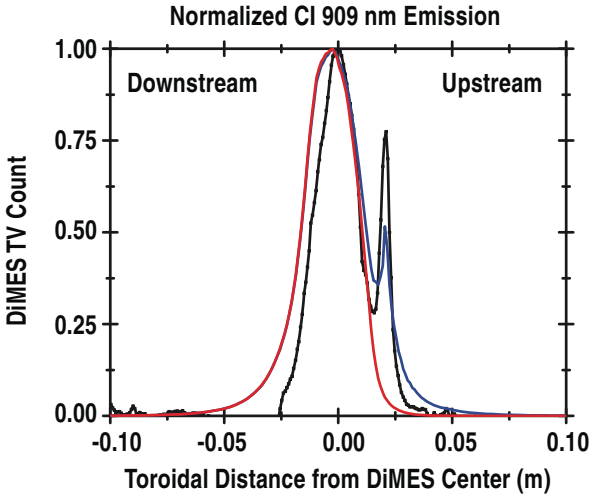

Fig. 5. CI 909 nm profile comparison. Shot 129060. Other details as Fig 3.

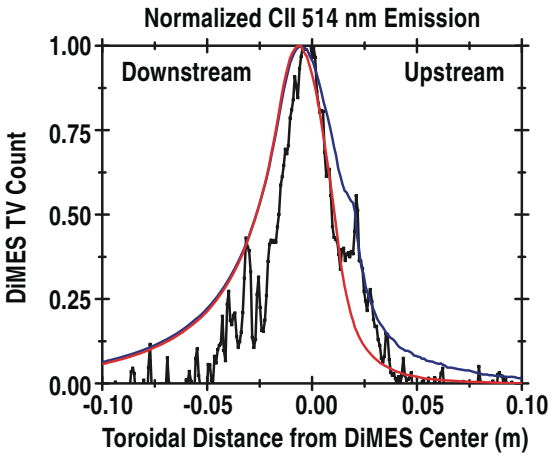

Fig. 6. CII 514 nm profile comparison. Shot 129691. Other details as Fig 3.

B. The absolute emissivity for five spectroscopic bands/lines

Absolute emission intensities of CH 0-0 band, CI 909 nm, CII 427 nm, 514 nm and 658 nm were measured using MDS which views a 2.1 cm diameter circle centered on the DiMES sample. The PPI particle source on DiMES is 3 cm across. As a result, the MDS views only regions which are the source of the puff. MDS background subtraction used the emission measured simultaneously on another MDS chord viewing at the same radial location but displaced toroidally. Comparisons with the code are shown in Table I. The absolute magnitudes agree to within a factor of roughly two for CH, CI, and CII 658 nm emissions. The modeled CII 427 nm emission is about 1/4 of the experimental value; this is attributed here to the contribution of excited C^+ created directly by the CH_4 breakup [9] (Sec. III-3). The modeled CII 514 nm emission is also smaller than the experimental value but by a smaller factor; because the background plasma conditions used in the simulations are directly from the LP data (which have an uncertainty of $\sim 2X$) and ionization rates and photon efficiencies are fairly sensitive to the local plasma density and temperature, varying the plasma conditions within the experimental uncertainties of measurement has a significant effect on the absolute emissions. This effect is investigated and found to be capable of explaining this discrepancy, i.e. it is just within the estimated uncertainties [4].

In summary, based on the combination of the JR hydrocarbon breakup model and the Jacob hydrocarbon sticking coefficient model 3D-DIVIMP(HC) calculates that 2.6 carbon atoms, in all atomic and molecular forms, enter the plasma for each CH_4 molecule initially injected (C recycling). The additional 1.6 carbon atoms are the result of surface interactions of fragments of the initially injected CH_4 molecule. Altogether, 57% of injected methane molecules have at least one interaction with the surface at some point in the break-up chain. This is a direct result of the Jacob hydrocarbon reflection model.

TABLE I. Comparison of measured (MDS) and code-calculated absolute emissivities. Measurement uncertainties are a factor of ~2.

	CH 427.0-431.5 nm	CI 910.0 nm	CII 426.7 nm	CII 514.0 nm	CII 658.0 nm
MDS L5 ($\times 10^{13}$ photons/cm^2/s/sr)*	7.4	2.5	3.0	8.7	10.5
3D-DIVIMP-HC ($\times 10^{13}$ photons/cm^2/s/sr)	10.8	6.2	0.76	2.6	6.4

* the MDS measured emissivities quoted here include both new calibrations and revised shot-to-shot analysis methods [2], compared with those in [11].

C. CII 427 nm emission from excited C^+ ions resulted from hydrocarbon breakup

Varying the parameters in the simulation did not quite resolve the discrepancy of the CII 427 nm absolute emissivity between the code and the experimental measurements. Janev and Reiter [9] suggested that a resonant transition due to electron collisions between the $1s^2 2p^3$ and the $1s^2 2s^2 4f$ states is fast, thus the $1s^2 2p^3$ state primarily decays via the $1s^2 2s^2 4f$ state. Therefore, two types of CII 427 nm emission may be considered: (a) the usual 'non-resonant' one where the population of the upper state of the CII 427 nm emission results from electron impact excitation of ground state C^+ to the $1s^2 2s^2 4f$ state, and (b) due to 'near-resonant excited' C^+ created by the breakup reaction $CH + e \rightarrow C^+ + H + 2e$ with the C^+ being created primarily in the $1s^2 2p^3$ state.

For CII 427 nm, the ADAS S/XB values for the PPI plasma condition is ~ 40. This means that $\sim 1 / 40 = 2.5\%$ C^+ produced by the normal (non-resonant) processes emits 1 photon at 427 nm. The simulation shows that $\sim 6.5\%$ of C^+ is produced from the reaction $e + CH \rightarrow C^+ + H + 2e$, using the JR model for the PPI plasma conditions. Thus an enhancement of the CII 427 nm emission by a factor of $\sim (0.065 + 0.025) / 0.025 \sim 3.6X$ would be expected on the basis of the above considerations. As noted earlier (Table 1), the measured emission was $3.0 \pm 0.6 \times 10^{13}$ ph/cm^2/s/sr while the simulation (based on non-resonant excitation) gave 0.76×10^{13} ph/cm^2/s/sr, a factor of ~ 4X. Thus this explanation suggested by Janev and Reiter appears to be capable of explaining this discrepancy to within the uncertainties.

D. The major reactions of the Janev-Reiter model for the PPI MkII plasma condition

So far all the simulations presented have utilized the full JR hydrocarbon breakup model, composed of 81 reactions in 6 categories. Presumably the most important

contributing reaction to a product and the most important evolving reaction from a reactant are the most essential reactions in the total reaction system. Based on these most essential reactions, detailed 3D-DIVIMP(HC) simulations show that in fact the simple 7-reaction sub-set:

$$CH_4 \xrightarrow{(33)} CH_3 \xrightarrow{(37)} CH_2 \xrightarrow{(5)} CH_2^+ \xrightarrow{(70)} CH \xrightarrow{(2)} CH^+ \xrightarrow{(76)} C \xrightarrow{(1)} C^+$$

gives only ~ 1.5X worse agreement with the measured emissivities, compared with an order of magnitude simplification in the model. This simple reaction chain is therefore a useful, approximate model for the breakup of methane in attached divertor tokamak plasma conditions. Future basic studies, experimental and theoretical, directed at improving the accuracy of the rates for methane breakup reactions would therefore be most usefully focused on these particular reactions. It should be noted that an important superiority of the full 81-reaction JR set over the reduced reaction set is that the simplified model does not include the special reaction, $e + CH \rightarrow C^+ + H + 2e$, the source of near-resonant excited C^+ that generates the excessive CII 427 nm emission when decaying to the ground state.

III. MODELING THE MISALIGNED PPI HEAD LEADING EDGE

Due to a slight misalignment of the PPI puff head (it was evidently inserted too far, by ~ 0.3 mm, Fig. 4) the plasma strongly interacted with the leading edge of the head facing the upstream direction, while the trailing edge of the head was "shielded" from any plasma contact in the downstream direction. This is apparent from Fig. 1. Natural physical and chemical sputtering occurred at this leading edge and were observed by the cameras. This emission could not be excluded by subtracting the background emission due to the interaction between the divertor floor tiles and the plasma (unfortunately no plasma discharges in which the DiMES sample was inserted without puffing CH_4 gas were measured).

A 3D-DIVIMP(HC) case was run, using the lab-measured chemical sputtering yields [10] and the physical sputtering yields [11], with the spatially constant plasma condition of 20 eV, 1.2×10^{19} m^{-3} to simulate the edge sputtering, in which two groups of particles are launched uniformly across the leading edge region to represent the physically and chemically sputtered source: 1) 8.7×10^{16} C are launched using a Thompson energy distribution for the physically sputtered particles, and 2) 5.6×10^{16} CH_4 are launched at 0.2 eV representing the chemically sputtered particles, using a 3D-cosine angular distribution with launch-axis pointed $45°$ up in the toroidal (upstream) direction (the angle of the bevel on the edge of the PPI head). The simulated toroidal profiles are compared with those measured by DiMES TV in Figs. 3, 5, and 6, which shows that 1) the relative intensity of the edge peak caused by the misalignment compared with the center peak caused mainly by the puff for the DiMES TV measurement (black) and the 3D-DIVIMP(HC) simulation (blue) is within a factor of 2X; 2) the relative positions of these two peaks also agree very well. It is therefore concluded that the hypothesis that the edge emission is caused by the PPI head misalignment is confirmed within the uncertainties.

IV. CONCLUSIONS

The Janev-Reiter methane breakup model/database, combined with the Jacob hydrocarbon reflection coefficients, as well as the neutral and ionic transport modeling in the new, full 3D, localized computer 3D-DIVIMP(HC) code, successfully replicates the DiMES TV-measured spatial shapes of the CH 427.0 – 431.5 nm, CI 909 nm, and CII 514 nm emission 'clouds' and the MDS-measured absolute magnitudes of CH 427.0 – 432.5 nm, CI 909 nm, CII 514 nm, and CII 658 nm emissions within the combined experimental uncertainty. Based on the usual assumption of electron impact excitation from the ground state, the code underestimated the CII 427 nm absolute emission by a factor of ~ 4; the $CH + e \rightarrow C^+ + H + 2e$ reaction, however, is known to produce excited C^+ in the $^2P^0$ state which is very close to $1s^2 2s^2 4f$, the upper state of the CII 427 nm transition, resulting in resonant excitation. When this was included in the code, close agreement was obtained with the measurement. It is therefore concluded that the simulation results are consistent with the general understanding of the controlling physics of attached divertor plasmas; the analysis is also consistent with and thus confirmatory of the lab-measured chemical and physical sputtering yields; the parallel ion transport is dominated by the frictional force, as expected for attached divertor conditions where parallel temperature gradient forces should be weak. The analysis tested the Janev-Reiter methane breakup model and the Jacob hydrocarbon reflection coefficient model, confirming that these models are correct within experimental uncertainty, for basic divertor conditions, namely attached, non-ELMing plasmas.

It is also shown that the reduced (from 81) simple reaction sub-set: $CH_4 \rightarrow CH_3 \rightarrow CH_2 \rightarrow CH_2^+ \rightarrow CH \rightarrow CH^+ \rightarrow C \rightarrow C^+$ gives results which are only slightly outside the estimated combined uncertainties. Hence these simple reaction chains are useful in providing rough pictures of the breakup of methane in attached divertor tokamak plasmas and therefore are the ones most worth focusing on in future work, theoretical or experimental, aimed at improving the reliability and accuracy of the methane breakup reactions – at least for attached plasma conditions.

REFERENCES

[1] A.G. McLean, *et al.*, J. Nucl. Mater. **363-365**, 86 (2007).

[2] C.P.C. Wong, R. Junge, R.D. Phelps, *et al.*, J. Nucl. Mater. **196–198**, 871 (1992).

[3] A.G. McLean, "Quantification of chemical erosion in the divertor of the DIII-D tokamak," University of Toronto PhD thesis, May 2009.

[4] Y. Mu, "Development and Applications of 3D-DIVIMP(HC) Monte Carlo Modeling Code," University of Toronto PhD thesis, November 2009.

[5] R.K. Janev and D. Reiter, Phys. Plasmas **9**, 4071 (2002).

[6] R.K. Janev and D. Reiter, J. Nucl. Mater. **313-316**, 1202 (2003).

[7] R.K. Janev and D. Reiter, "Collision processes of hydrocarbon species in hydrogen plasmas: I. The methane family," Report FZ-Jülich Jül -3966, Forschungszentrum Jülich, Jülich Germany (Feb. 2002).

[8] W. Jacob, J. Nucl. Mater. **337-339**, 839-846 (2005).

[9] D. Reiter and P.C. Stangeby (private communication).

[10] B.M. Mech, *et al.*, J. Nucl. Mater. **255**, 153 (1998).

[11] S. Brezinsek, *et al.*, "Spectroscopic studies of carbon sources in present tokamaks," 30th EPS Conference on Contr. Fusion and Plasma Phys., St. Petersburg, 7-11 July 2003 ECA Vol. **27A**, O-2.4D.

[12] Y. Mu, *et al.*, J. Nucl. Mater. **390-391**, 220 (2009).

ACKNOWLEDGMENTS

This work was supported in part by the U.S. Department of Energy under DE-FC02-04ER54698, DE-FG02-04ER54758, DE-FG02-07ER54917, and DE-AC05-00OR22725. The authors would like to acknowledge the DIII-D Team for their continued efforts in assisting our experiments and providing long time support, in particular, the DIII-D DiMES Group, including B.D. Bray, N.H. Brooks, J.W. Davis, M.E. Fenstermacher, M. Groth, C.J. Lasnier, D.L. Rudakov, J.G. Watkins, W.P. West, and C.P.C. Wong. Support by the Natural Sciences and Engineering Research Council of Canada is acknowledged.